

ChemComm

Accepted Manuscript



This is an *Accepted Manuscript*, which has been through the Royal Society of Chemistry peer review process and has been accepted for publication.

Accepted Manuscripts are published online shortly after acceptance, before technical editing, formatting and proof reading. Using this free service, authors can make their results available to the community, in citable form, before we publish the edited article. We will replace this *Accepted Manuscript* with the edited and formatted *Advance Article* as soon as it is available.

You can find more information about *Accepted Manuscripts* in the [Information for Authors](#).

Please note that technical editing may introduce minor changes to the text and/or graphics, which may alter content. The journal's standard [Terms & Conditions](#) and the [Ethical guidelines](#) still apply. In no event shall the Royal Society of Chemistry be held responsible for any errors or omissions in this *Accepted Manuscript* or any consequences arising from the use of any information it contains.



Journal Name

COMMUNICATION

Durable and Self-Healing Superamphiphobic Coatings Repellent Even towards Hot Liquids

Received 00th January 20xx,
Accepted 00th January 20xx

Bucheng Li, and Junping Zhang*

DOI: 10.1039/x0xx00000x

www.rsc.org/

Durable and self-healing superamphiphobic coatings with high repellency to both cool and hot liquids are successfully prepared on various substrates by the combination of rodlike palygorskite and organosilanes via spray-coating. The coatings feature high mechanical, environmental and chemical durability, and are self-healing.

Superamphiphobic surfaces repellent to both water and organic liquids have generated extensive attention.¹ Different from superhydrophobic surfaces, the creation of superamphiphobic surfaces is difficult because of the low surface tension of organic liquids compared to water.^{1,2} According to Young's equation, the lower the surface tension, the higher the tendency of a liquid to spread on a solid surface.³ Although various methods have been used,¹ most superamphiphobic surfaces only repel liquids with surface tension above 27.5 mN m⁻¹ (*n*-hexadecane). In addition, organic liquids often have high contact angles (CAs ≥ 150°) but adhere stably on the surface and cannot roll off, which means lack of the important self-cleaning property.⁴ It is still very challenging to create superamphiphobic surfaces on which liquids of low surface tension could roll off easily with low sliding angles (SAs) because the liquid-solid interaction should be very weak.⁵ Both special microstructures (e.g., re-entrant curvatures, overhang structures, silicone nanofilaments and fabrics)^{2,6} and materials of very low surface energy (e.g., fluorodecyl POSS) are necessary to achieve low SAs. However, most methods are complicated, expensive and limited to specific substrates, which hamper their applications.

Moreover, the practical use of superhydrophobic and superamphiphobic surfaces in real-life conditions is severely limited by durability issues.⁷ Most superamphiphobic surfaces can be easily damaged by mechanical abrasion, harsh environment and corrosive substances, etc. With the experience of designing durable

superhydrophobic surfaces,⁸ durable superamphiphobic surfaces may be prepared by enhancing stability of the microstructure, making the surface self-healing, and preserving both the microstructure and low surface energy.^{3,9}

Further, the existing superamphiphobic surfaces are only repellent to cool liquids (~25 °C). To the best of our knowledge, there is no superamphiphobic surface repellent to hot organic liquids. It was reported that most superhydrophobic surfaces, both natural and artificial, lose superhydrophobicity when exposed to hot water.¹⁰ Although the reasons are not entirely clear, the condensation of water vapor between hot water and superhydrophobic surfaces, due to their temperature difference, is responsible for the loss of superhydrophobicity.¹⁰ Water vapor could easily get into the micro-/nano-pores of superhydrophobic surfaces and induce the increase of the liquid-solid contact area, which results in adhesion of water on the surfaces. The lower surface tension of water at high temperature also contributes to the loss of superhydrophobicity.¹¹ Superamphiphobic surfaces repellent to hot liquids are in a high demand, and will have wide applications in many fields, e.g., hot liquids transportation, scalding protection clothes and heat transfer, etc.

Herein, we report a simple spray-coating approach for the fabrication of durable and self-healing superamphiphobic coatings repellent to both cool and hot liquids by the combination of palygorskite (PAL), 1*H*,1*H*,2*H*,2*H*-perfluorodecyltriethoxysilane (PFDTES) and tetraethoxysilane (TEOS) (Fig. 1a). Clay minerals are natural nanomaterials frequently used for the reinforcement of polymers because of their high performance and low cost,¹² but are not yet used for designing superamphiphobic coatings. In fact, PAL, a crystalline hydrated magnesium aluminum silicate with a rodlike microstructure (Fig. 1b),¹² is a very promising building block for the design of superamphiphobic coatings. Coatings based on organosilanes are well known because of their fine properties and simplicity.¹³ We have prepared superhydrophobic and superamphiphobic coatings with excellent properties using organosilanes.^{2,14} Compared to the existing superamphiphobic coatings, the coatings reported here have the following advantages. (1) The coatings are prepared using inexpensive PAL via a simple strategy and are applicable on various substrates. The introduction

B. C. Li, Prof. J. P. Zhang
Center of Eco-material and Green Chemistry
Lanzhou Institute of Chemical Physics, Chinese Academy of Sciences
730000, Lanzhou, P.R. China
Email: jpzhang@licp.cas.cn

† Footnotes relating to the title and/or authors should appear here.

Electronic Supplementary Information (ESI) available: [Experimental section, spectra, analytical data, images and videos]. see DOI: 10.1039/x0xx00000x

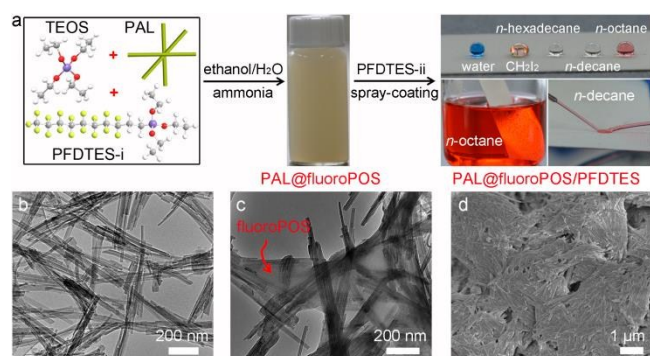


Fig. 1. (a) Preparation of PAL@fluoroPOS and superamphiphobic PAL@fluoroPOS/PFDTES coatings, (b) TEM image of PAL, (c) TEM image of PAL@fluoroPOS and (d) SEM image of the PAL@fluoroPOS/PFDTES coating.

of PAL reduced the cost of superamphiphobic coatings by 40% compared to those based on fluorodecyl POSS.^{6a,9} (2) The coatings show excellent superamphiphobicity for both cool liquids and hot liquids. (3) The coatings feature high mechanical, environmental and chemical durability, and are self-healing.

Fig. 1a describes the strategy for preparation of the superamphiphobic coatings. First, PAL@fluorinated polysiloxane (PAL@fluoroPOS) was prepared by hydrolytic co-condensation of PFDTES and TEOS in the presence of PAL. In an ethanol-water solution with ammonia as the catalyst, PFDTES and TEOS gradually co-condensed onto the PAL crystals to form PAL@fluoroPOS. Subsequently, the superamphiphobic PAL@fluoroPOS/PFDTES coatings were prepared by spray-coating the homogeneous suspensions of the mixtures of PAL@fluoroPOS and PFDTES onto various substrates. Random deposition of the PAL crystals builds the “skeleton” of the coating with a rough topography at the surface. FluoroPOS links the PAL crystals together and makes surface energy of the coating very low. PFDTES forms additional crosslinking points with fluoroPOS to make the coating more durable, and also acts as the healing agent embedded in the coating.

PAL@fluoroPOS is highly dispersible in ethanol. The PAL crystals in PAL@fluoroPOS are linked together by fluoroPOS (Fig. 1c). No silica nanoparticle was observed in PAL@fluoroPOS, whereas a lot of nanoparticles were formed in the absence of PAL (Fig. S1). This is because PAL crystals induced co-condensation of PFDTES and TEOS by forming Si-O-Si bonds (Fig. S2). The PAL@fluoroPOS/PFDTES coatings have a compact and rough topography at the surface (Fig. 1d). The PAL crystals are tightly linked together by fluoroPOS and PFDTES. Without PFDTES, the PAL crystals are loosely linked by fluoroPOS (Fig. S3). XPS analysis confirmed the presence of C, O, F and Si on the surface of the coating with a C/O/F/Si atomic ratio of 1:0.74:1.90:0.40 (Fig. S4), and is consistent with the EDS result (Fig. S5). The F 1s peak is very strong, and the CF₂ (291.3 eV) and CF₃ (293.8 eV) peaks can be easily recognized in the C 1s spectrum, which indicate very high F content (46.97 at.%) on the surface of the coating. Also, the coating is homogeneous verified by the C, O, F and Si elemental maps (Fig. S6).

Wettability of the PAL@fluoroPOS/PFDTES coatings depends on topography and chemical composition of the coatings, which can be regulated simply by the concentrations of PAL (C_{PAL}), PFDTES

($C_{\text{PFDTES-i}}$) and TEOS (C_{TEOS}) in preparation of PAL@fluoroPOS as well as the spray-coating conditions.

The $CA_{n\text{-decane}}$ increased significantly from 57° to 156° with increasing C_{PAL} from 0 to 10 g L⁻¹, and remained constant with further increasing C_{PAL} to 20 g L⁻¹ (Fig. S7). With a C_{PAL} of 5 g L⁻¹, the *n*-decane droplets adhered strongly on the coating although the $CA_{n\text{-decane}}$ was ~150°, indicating that the droplets are in the Wenzel state. This is the frequently observed phenomenon for most existing superamphiphobic coatings.^{4, 15} The $SA_{n\text{-decane}}$ suddenly decreased to 9° with increasing C_{PAL} to 10-20 g L⁻¹, indicating transition from the Wenzel state to the Cassie-Baxter state. It was found that the behavior of *n*-decane droplets on the coatings is closely related to topography of the skeleton built using the PAL crystals, which can be regulated by changing C_{PAL} (Fig. S8). Without PAL, a smooth oleophilic coating was formed. With a C_{PAL} of 5 g L⁻¹, a rough coating was formed, but most PAL crystals were embedded in fluoroPOS. Such topography is sufficient to support the *n*-decane droplets in the Wenzel state. Upon increasing C_{PAL} to 10 g L⁻¹, a dramatic change of surface topography was observed. The PAL crystals were loosely linked together by fluoroPOS, which means an evident increase of surface roughness. Such topography could trap more air beneath the droplets and successfully alter the *n*-decane droplets to the Cassie-Baxter state. Upon further increasing C_{PAL} to 15 g L⁻¹, the PAL crystals were only stacked together, which is disadvantageous to durability of the coating although has no influence on superamphiphobicity. The great influence of PAL on superamphiphobicity inspired us to study the effects of other clay minerals with different microstructures. Sepiolite with a fibrous microstructure similar to PAL can also form superamphiphobic coatings with a large $SA_{n\text{-octane}}$, whereas only oleophobic coatings were formed in the case of halloysite (nanotubes) and Na⁺-montmorillonite (nanoplatelets) (Table S1).

PAL became oleophobic after coated with PFDTES and TEOS owing to the perfluorodecyl groups (Fig. S9). The $CA_{n\text{-octane}}$ was zero at a $C_{\text{PFDTES-i}}$ of 6.3 mM, and sharply increased to ~150° in the range 12.6-27.2 mM $C_{\text{PFDTES-i}}$. The *n*-octane droplets pinned stably on the coating at a $C_{\text{PFDTES-i}}$ of 12.6 mM, and the $SA_{n\text{-octane}}$ decreased to 20.6° with further increasing $C_{\text{PFDTES-i}}$ to 25.2 mM. A small amount of TEOS (4.5 mM) had no influence on the $CA_{n\text{-decane}}$, but decreased the $SA_{n\text{-decane}}$ from 26° to 10° (Fig. S10). TEOS, a coupling agent, is helpful for the hydrolytic condensation of PFDTES on the surface of PAL. Consequently, the PAL crystals were linked together by fluoroPOS, and a skeleton with improved surface topography was formed (Fig. S11a-b). With further increasing C_{TEOS} to 26.9 mM, the $CA_{n\text{-decane}}$ slightly decreased to 149° and the $SA_{n\text{-decane}}$ increased to 29°, and finally the droplets pinned stably on the coating. The excess TEOS further increased roughness of the coating (Fig. S11c-d), but resulted in deterioration of the superamphiphobicity owing to hydrophilic nature of the hydrolytic product of TEOS.

It should be noted that coatings with comparable superamphiphobicity can be also fabricated by spray-coating the PAL@fluoroPOS suspension (Fig. S12). However, the mixtures of PAL@fluoroPOS and PFDTES were used in order to make the coatings more durable by forming additional crosslinking points with fluoroPOS (Fig. S2) and to make the coatings self-healing. Different from the PAL@fluoroPOS coating composed of loosely linked PAL crystals (Fig. S13a), the PAL@fluoroPOS/PFDTES coatings

had a compact and rough topography at the surface (Fig. S13b-d). The PAL crystals were tightly linked together by fluoroPOS and PFDTES. A $C_{\text{PFDTES-ii}}$ of 0–22.6 mM had no influence on the $CA_{n\text{-decane}}$, but the $SA_{n\text{-decane}}$ slightly increased from 9° to 14° at a $C_{\text{PFDTES-ii}}$ of 17.0–22.6 mM (Fig. S12). This is because the excess PFDTES decreased surface roughness of the coating.

After confirming the relationship between preparation parameters, surface topography and chemical composition, and wettability, superamphiphobicity of the coating was tested by recording CAs, SAs and kinetic behaviors of various typical liquids with different surface tension. All the liquids investigated, even *n*-octane, were spherical in shape with high CAs and low SAs (Fig. 1a and Table S2). The droplets could easily roll off the tilted coating owing to the existence of the air cushion between the coating and the droplets.¹⁶ The coating was reflective in *n*-octane with a silver mirror-like surface and remained completely dry after taken out of *n*-octane to air (Fig. 1a), which were direct evidences for the existence of the air cushion. This means that most area beneath the droplet is the liquid-vapor interface, and the liquid-solid interaction is very weak. This is further verified by jetting of *n*-decane on the coating. The PAL@fluoroPOS/PFDTES coatings with comparable superamphiphobicity are also applicable onto other substrates, e.g., wood plate, aluminum plate and polyester textile, etc., regardless of composition and topography of the substrates (Fig. S14 and Table S3). The coating also showed self-cleaning property (Fig. S15). All the liquids listed in Table S2 can be used to efficiently remove powdered dirt on the coating. This is attributed to the weak interaction of the coating with liquid droplets and the dirt as well as the rolling motion of droplets on the coating.

Most superhydrophobic surfaces lose superhydrophobicity once exposed to hot water.¹⁰ The CA_{water} on lotus leaves dropped to ~40° with increasing water temperature to 55 °C.¹¹ Different from previous superhydrophobic and superamphiphobic coatings, the PAL@fluoroPOS/PFDTES coating showed excellent superamphiphobicity not only for cool liquids, but also for hot liquids. The changes of the CAs and SAs of various liquids with liquid temperature are shown in Fig. 2a-b. The CAs of all the liquids decreased gradually with the increase of temperature to 85 °C. The CA_{water} , $CA_{\text{diiodomethane}}$ and $CA_{n\text{-hexadecane}}$ were above 150°, but the

$CA_{n\text{-dodecane}}$ decreased to 137° at 85 °C. The SA_{water} and $SA_{\text{diiodomethane}}$ remained below 4° in the range 25–85 °C. The $SA_{n\text{-hexadecane}}$ increased gradually to 9° at 70 °C and further increased to 18° at 85 °C. All the water, diiodomethane and *n*-hexadecane droplets in the range 25–85 °C could roll off the tilted coating, which means that the hot droplets are also in the Cassie-Baxter state. Jets of 94 °C water and 70 °C *n*-hexadecane could bounce off the coating without leaving a trace (Fig. 2c-d, Movie S1), indicating excellent repellency to hot liquids. The $SA_{n\text{-dodecane}}$ increased to 21° at 50 °C; further increase to 70 °C resulted in adhesion of the droplets on the coating although the $CA_{n\text{-dodecane}}$ was as high as 150°. This means the *n*-dodecane droplets have changed to the Wenzel state (inset in Fig. 2a). In spite of gradual decline, the coating still kept excellent superamphiphobicity for hot liquids up to 85 °C. This is attributed to the compact topography and very low surface energy of the coating, which reduced the condensation of liquid vapor on the coating, and then hindered the increase of the liquid-solid contact area.

Although superamphiphobic coatings with low SAs for liquids with surface tension below 27.5 mN m⁻¹ have been successfully created on smooth surfaces,^{6a-c} low durability of superamphiphobic coatings is an issue widely concerned. Regarding durability and self-healing ability of the PAL@fluoroPOS/PFDTES coating, a series of experiments has been carried out.

Mechanical durability of the coating was investigated by the water jetting test (Figs. 3a and S16), a commonly used method in which a jet of water with controlled pressure hits the coating.¹⁷ The introduction of PFDTES into the spray-coating suspension remarkably improved mechanical durability of the coating by forming additional crosslinking points (Fig. 3b). Compared to the other coatings, the coating with a $C_{\text{PFDTES-ii}}$ of 11.3 mM showed the highest durability in the water jetting test. The $SA_{n\text{-decane}}$ remained as low as 15° and the coating was dry after intensive jetting at 100 kPa for 10 min (velocity of 14.1 m s⁻¹, Movie S2). In addition, only slight decrease of the $CA_{n\text{-decane}}$ to 153° was detected after jetting for 10 min regardless of $C_{\text{PFDTES-ii}}$. Durability of the coating to water jetting depends on water pressure and jetting time. Although the $CA_{n\text{-decane}}$ decreased and the $SA_{n\text{-decane}}$ increased with increasing pressure and time (Figs. S17 and S18), the coating maintained superamphiphobicity after jetting up to 150 kPa for 30 min (velocity of 17.3 m s⁻¹). The water impacted the coating at twice the velocity of heavy rain (8–9 m s⁻¹) and more than ten times the water velocity reported for evaluating mechanical durability of superamphiphobic coatings (1.4 m s⁻¹).³ The coating remained dry, the $CA_{n\text{-decane}}$ was 150° and the $SA_{n\text{-decane}}$ was 34° after jetting at 150 kPa for 30 min. No change in topography of the coating was observed after jetting at 150 kPa for 30 min (Fig. 3c). Mechanical durability of the coating was also tested via the other two complementary tests, peeling with an adhesive tape and finger press (Fig. S19). The adhesive tape was pressed with ~10 kPa to the coating, and then peeled off. Repeated peeling with the new tape had no influence on the $CA_{n\text{-decane}}$, and resulted in gradual increase in the $SA_{n\text{-decane}}$. The coating remained superamphiphobic ($CA_{n\text{-decane}}$ = 154°, $SA_{n\text{-decane}}$ = 15.2°) after pressed with finger for 50 times (~10 kPa).

The high environmental and chemical durability of the coating was also demonstrated (Table S4). The coating was stable under UV irradiation and harsh temperatures. The $CA_{n\text{-decane}}$ and $SA_{n\text{-decane}}$ remained constant after kept in liquid N₂ (Fig. 3d) and at

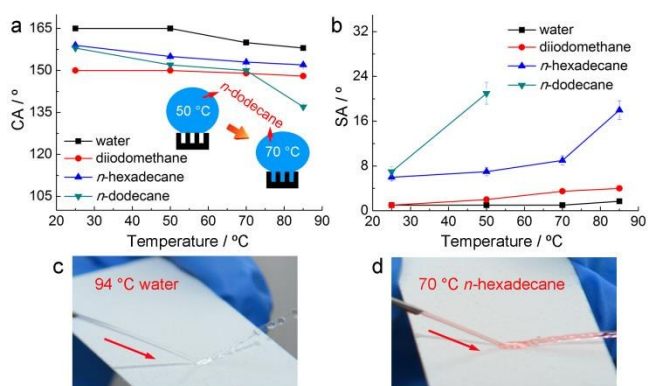


Fig. 2. Variation of (a) CAs and (b) SAs of various liquid droplets (5 μL) with their temperature on the PAL@fluoroPOS/PFDTES coating, and images of the coating with a jet of (c) hot water and (c) hot *n*-hexadecane bouncing off.

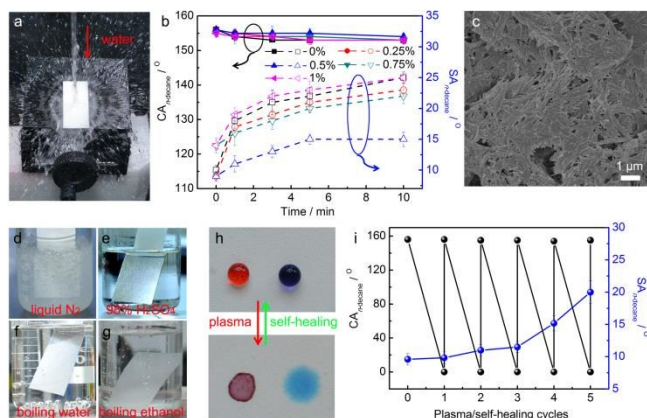


Fig. 3. (a) Image of water jetting test at 100 kPa, (b) effects of $C_{\text{PFDTES-II}}$ on $CA_{n\text{-decane}}$ and $SA_{n\text{-decane}}$ in the water jetting test at 100 kPa, (c) SEM image of the PAL@fluoroPOS/PFDTES coating after water jetting at 150 kPa for 30 min, (d-g) images of the coating immersed in various liquids, (h) images of water (blue) and n -decane (red) droplets on the coating in the plasma/self-healing test and (i) $CA_{n\text{-decane}}$ and $SA_{n\text{-decane}}$ changes in the plasma/self-healing test.

temperature up to 350 °C for 1 h (Fig. S20). The coating was also resistant to corrosive liquids (1 M $\text{HCl}_{(\text{aq})}$, 1 M $\text{NaOH}_{(\text{aq})}$, saturated $\text{NaOH}_{(\text{aq})}$ and saturated $\text{NaCl}_{(\text{aq})}$) and organic solvents (n -octane and toluene). No changes of the $CA_{n\text{-decane}}$ and $SA_{n\text{-decane}}$ were detected after immersed in these liquids for 1 h. Immersion in 98% H_2SO_4 for 1 h had no effect on the $CA_{n\text{-decane}}$ and only resulted in increase of the $SA_{n\text{-decane}}$ to 17°. In addition, the coating retained its superamphiphobicity even after boiled in water and ethanol for 1 h although the $SA_{n\text{-decane}}$ increased to 20–24° (Fig. 3f-g). Moreover, immersion in water for 240 h has negligible influence on superamphiphobicity of the coating (Fig. S21). Except for liquid N_2 and boiling ethanol, the air cushions between the coating and various liquids in Table S4 were maintained (Fig. 3e-f and Movie S3), indicating high environmental and chemical durability of the coating.

The superamphiphobic PAL@fluoroPOS/PFDTES coating became superhydrophilic/superoleophilic after air plasma treatment (Fig. 3h). Interesting, the damaged coating is self-healing under room conditions in 24 h. This is different from the previous studies in which special conditions, e.g., high humidity and heat treatment, are necessary for recovery of the damaged superhydrophobic and superamphiphobic coatings. No obvious change in the $CA_{n\text{-decane}}$ was observed and the $SA_{n\text{-decane}}$ increased to 20° in the five plasma/self-healing cycles (Fig. 3i). Once damaged, the PFDTES molecules preserved in the coating spontaneously migrated to the surface of the coating via thermal motion and the damaged areas with hydrophilic groups were buried inside the coating to lower the surface energy.^{8b} XPS analysis of the coating after five plasma/self-healing cycles confirmed this deduction (Fig. S22). In this way, the damaged coating perfectly self-healed.

In summary, we have successfully fabricated superamphiphobic coatings with high CAs and low SAs for both cool and hot liquids by the combination of PAL and organosilanes using a simple spray-coating method. The topography and chemical composition of the coating play important roles in influencing the superamphiphobicity, and can be regulated simply by the concentrations of PAL, PFDTES and TEOS in preparation of PAL@fluoroPOS. Furthermore, the

superamphiphobic coatings show high mechanical, environmental and chemical durability, and are self-healing. We believe that the superamphiphobic coatings could be applied to various fields, as the coatings can be easily formed on various substrates by a very simple procedure. We anticipate that our findings may shed light on the design of novel superamphiphobic coatings repellent to hot liquids.

We are grateful for financial support of the “Hundred Talents Program” of the Chinese Academy of Sciences and the National Natural Science Foundation of China (51503212).

Notes and references

- [1] Z. Chu and S. Seeger, *Chem. Soc. Rev.*, 2014, **43**, 2784.
- [2] J. P. Zhang and S. Seeger, *Angew. Chem. Int. Ed.*, 2011, **50**, 6652.
- [3] X. Deng, L. Mammen, H. J. Butt and D. Vollmer, *Science*, 2012, **335**, 67.
- [4] a) J. Zimmermann, M. Rabe, G. R. J. Artus and S. Seeger, *Soft Matter*, 2008, **4**, 450; b) T. Darmanin and F. Guittard, *J. Am. Chem. Soc.*, 2009, **131**, 7928.
- [5] K. Tsujii, T. Yamamoto, T. Onda and S. Shibuichi, *Angew. Chem. Int. Ed.*, 1997, **36**, 1011.
- [6] a) A. Tuteja, W. Choi, M. Ma, J. M. Mabry, S. A. Mazzella, G. C. Rutledge, G. H. McKinley and R. E. Cohen, *Science*, 2007, **318**, 1618; b) T. Y. Liu and C. J. Kim, *Science*, 2014, **346**, 1096; c) M. Zhang, T. Zhang and T. Cui, *Langmuir*, 2011, **27**, 9295; d) H. Zhou, H. X. Wang, H. T. Niu, J. Fang, Y. Zhao and T. Lin, *Adv. Mater. Interfaces*, 2015, **2**, 1400559.
- [7] a) H. Jin, X. Tian, O. Ikkala and R. H. Ras, *ACS Appl. Mater. Interfaces*, 2013, **5**, 485; b) S. A. Kulinich, S. Farhadi, K. Nose, and X. W. Du, *Langmuir*, 2011, **27**, 25; c) S. A. Kulinich, M. Honda, A. L. Zhu, A. G. Rozhin and X. W. Du, *Soft Matter*, 2015, **11**, 856.
- [8] a) T. Verho, C. Bower, P. Andrew, S. Franssila, O. Ikkala and R. H. Ras, *Adv. Mater.*, 2011, **23**, 673; b) Y. Li, L. Li and J. Sun, *Angew. Chem. Int. Ed.*, 2010, **49**, 6129.
- [9] H. Wang, Y. Xue, J. Ding, L. Feng, X. Wang and T. Lin, *Angew. Chem. Int. Ed.*, 2011, **50**, 11433.
- [10] F. Wan, D. Q. Yang and E. Sacher, *J. Mater. Chem. A*, 2015, **3**, 16953.
- [11] Y. Liu, X. Chen and J. H. Xin, *J. Mater. Chem.*, 2009, **19**, 5602.
- [12] J. Zhang, Q. Wang and A. Wang, *Carbohydr. Polym.*, 2007, **68**, 367.
- [13] L. Gao and T. J. McCarthy, *J. Am. Chem. Soc.*, 2006, **128**, 9052.
- [14] a) J. Zhang, B. Li, L. Wu and A. Wang, *Chem. Commun.*, 2013, **49**, 11509; b) J. P. Zhang, A. Q. Wang and S. Seeger, *Adv. Funct. Mater.*, 2014, **24**, 1074.
- [15] H. Li, X. Wang, Y. Song, Y. Liu, Q. Li, L. Jiang and D. Zhu, *J. Mater. Chem.*, 2001, **40**, 1743.
- [16] C. Luo, H. Zheng, L. Wang, H. Fang, J. Hu, C. Fan, Y. Cao and J. Wang, *Angew. Chem. Int. Ed.*, 2010, **49**, 9145.
- [17] a) D. Ge, L. Yang, Y. Zhang, Y. Rahmawan and S. Yang, *Part. Part. Syst. Char.*, 2014, **31**, 763; b) S. D. Wang and Y. S. Jiang, *Appl. Surf. Sci.*, 2015, **357**, 1647.